High Strength Nylon Micro- and Nanofiber Based Nonwovens via Spunbonding

Nataliya Fedorova, Behnam Pourdeyhimi

Nonwovens Cooperative Research Center, North Carolina State University, Raleigh, North Carolina 27695-8301

Received 22 April 2006; accepted 11 December 2006
DOI 10.1002/app.25939
Published online 8 March 2007 in Wiley InterScience (www.interscience.wiley.com).

ABSTRACT: In this study we explore the feasibility of using of islands-in-the-sea (I/S) fibers in the spunbond process to produce relatively high strength micro- and nanofiber webs. The relationships between the number of islands, percent polymer composition, and the fiber and fabric properties are reported. Nylon 6 (N6) and poly (lactic) acid (PLA) were used as the islands and sea polymers, respectively. Micro- and nanofibers were obtained by dissolving PLA polymer from the final spunbond nonwovens. The fibers with 25% N6 showed a decrease in fiber diameter from 1.3 to 0.36 μm (micron) when the number of islands was increased from 36 to 360. The diameter of fibers with 75% N6 showed a decline from 2.3 to 0.5 μm for the same range. Hydroentangling was found to be the preferred method of bonding of the I/S structures; the bonded structures were able to withstand postprocessing steps required for dissolving of the sea from the resulting nonwovens. Hydroentanged micro- and nanofiber based nonwovens demonstrated high tensile and tear properties, which were insensitive to the N6 fiber size and its mechanical properties. Bonding efficiency and web uniformity were found to be dominant factors influencing the fabric performance. Overall, our study demonstrated that the I/S configuration is a promising technique for high speed and high throughput production of strong and light weight nonwovens comprised of micro- and nanofibers. J Appl Polym Sci 104: 3434–3442, 2007

Key words: nanofibers; nylon 6; poly(lactic) acid; mechanical properties; spunbonding

INTRODUCTION

Fabrics composed of micro- or nanofibers offer small pore size and large surface area. Thus, they are expected to bring value to applications where such properties as sound and temperature insulation, fluid holding capacity, softness, durability, luster, barrier property enhancement, and filtration performance are needed. In particular, products intended for liquid and aerosol filtration, composite materials for protective gear and clothing, and high performance wipes could benefit greatly from the introduction of such small fibers.[1–8]

In the fiber industry, there is no commonly accepted definition of nanofibers. Some authors refer to them as materials with a diameter ranging from 0.1 to 0.5 μm (micron),[2] while others consider filaments smaller than 1 μm as nanofibers,[4,9] and some hold the opinion that nanofibers are materials with diameters below 0.1 μm.[10] Here, we will define nanofibers as fibers whose diameters measure 0.5 μm or less. Filaments with diameters ranging from 0.5 to 5 μm will be considered as microfibers.

Correspondence to: B. Pourdeyhimi (behnam_pourdeyhimi@ncsu.edu).

Contract grant sponsor: Nonwovens Cooperative Research Center.

Manufacturing techniques associated with the production of polymeric micro- and nanofibers are electrospinning, meltblowing and the use of ''splittable'' segmented pie or ''soluble'' islands-in-the-sea (I/S) bicomponent fibers. In electrospinning, a fiber is drawn from a polymer solution or melt by electrostatic forces.[11] This process is able to produce filaments with diameters in the range from 40 to 2000 nm (nanometers).[12] In meltblowing, melted polymers are extruded from dies, attenuated by heated, high velocity air streams, and spun into fibers having diameters in between 0.5 and 10 μm.[6,13–15] Even though filaments measuring 0.5 μm can be obtained via this technique, most commercially available meltblown media are generally about 2 μm and above.

''Splittable'' and ''soluble'' fiber technologies allow production of fibers with diameter ranging from 0.1 to 5 μm.[7,16] This is often accomplished through two steps: (1) spinning of the segmented pie or I/S bicomponent fibers via spunbonding, which involves extruding of polymer melts through dies, cooling, and attenuating of fibers by high velocity air streams; (2) releasing of small filaments by applying mechanical action, such as hydroentangling, carding, twisting, drawing etc. to the bicomponent fibers, or by dissolving one of the components.

In general, meltblowing and electrospinning produce nonwoven mats rather than single fibers and these mats consist of fibers characterized by low

TABLE I
Properties of Polymers Used

Polymer	Melting temperature, T_m (°C)	Density (g/cm^3)	Viscosity
N6	220	1.14	2.67 – 2.73[a]
PLA	173	1.25	N/A

[a] Relative viscosity measured at 1 % of solution in sulfuric acid (96%) at 25°C.

strength.[6,17–19] Thus, electrospun or meltblown fiber webs are typically laid over a suitable substrate that provides appropriate mechanical properties and complementary functionality to the fabric.[6] Moreover, existing meltblowing processes are not able to produce nanofiber webs easily, and they can process only a limited number of polymers.[20] Electrospinning, on the other hand, is able to make nanofiber mats with substantially smaller fibers than meltblown or spunbonded webs, however this process has very low productivity.[2,12,17]

We believe that the segmented pie and I/S fibers offer commercially viable alternatives to electrospinning or meltblowing. Products produced by using these fibers can be quite uniform and they can have sufficient strength to allow their use in various applications without a need for a carrier. A great example is the segmented pie microfiber product made by Freudenberg and marketed as Evolon®.[21]

The I/S approach can produce significantly smaller fibers than the segmented pie technique, however the sea in the I/S fibers has to be removed, and this often creates an environmental issue. Also, since virtually all spunbonds are thermally bonded, subsequent removal of the sea component from thermally bonded substrates could result in the loss of structure as a result of disintegration of the bond spots. Thus, I/S spunbond webs require an alternative means of bonding the structure in place of thermal bonding.

Because of all abovementioned, there are no commercial products available today based on the spunbond I/S technology. Nonetheless, we believe that I/S spunbond nonwovens offer significant promise for the production of large volumes of micro- and nanofiber webs.

The purpose of this study is to demonstrate the feasibility of using of the I/S fibers in the spunbond process for production of high strength micro- and nanofiber webs. The properties of the I/S fibers and fiber webs made up of Nylon 6 (N6) as the islands and poly (lactic) acid (PLA) as the sea were investigated and the relationships between the number of islands, polymer compositions, and the fiber and fabric properties were determined.

EXPERIMENTAL

Materials

Ultramid BS 700 nylon-6 (N6) (BASF) and poly(lactic) acid (PLA) (Nature Works LLC) were used as the island and sea polymers, respectively. Basic properties of these polymers are summarized in Table I.

Methods

Sample preparation

Homo-component and bicomponent spunbond fibers and webs were produced at Nonwovens Cooperative Research Center (NCRC) Pilot facilities located at North Carolina State University. Sample description is given in Table II. All webs were hydroentangled at a speed of 30 m/min. Hydroentangling was chosen as the preferred method for bonding of the I/S webs because fiber-to-fiber entanglement would not be lost by the removal of the sea and the web structure integrity would be maintained. The total hydroentangling energy required to entangle the webs was 8000 kJ/kg. Several sample sets were also additionally calendered at a temperature of 190 and 145°C prior and after PLA removal, respectively. Calender bonding for all samples was conducted at a speed of 15 m/min with a nip pressure of 70 kN/m (400 pounds per linear inch).

TABLE II
Description of the Nonwoven Samples Produced

Sample abbreviation	Sample type	No. of Islands	Polymer		Polymer ratio (%)	
			Island	Sea	Island	Sea
100% N6	Fibers	0	–	N6	–	100
100% PLA	Fibers	0	–	PLA	–	100
36 I/S 25/75 N6/PLA	Fibers & Fabrics	36	N6	PLA	25	75
36 I/S 75/25 N6/PLA	Fibers & Fabrics	36	N6	PLA	75	25
108 I/S 25/75 N6/PLA	Fibers & Fabrics	108	N6	PLA	25	75
108 I/S 25/75 N6/PLA	Fibers & Fabrics	108	N6	PLA	75	25
216 I/S 25/75 N6/PLA	Fibers & Fabrics	216	N6	PLA	25	75
216 I/S 25/75 N6/PLA	Fibers & Fabrics	216	N6	PLA	75	25
360 I/S 25/75 N6/PLA	Fibers & Fabrics	360	N6	PLA	25	75
360 I/S 25/75 N6/PLA	Fibers & Fabrics	360	N6	PLA	75	25

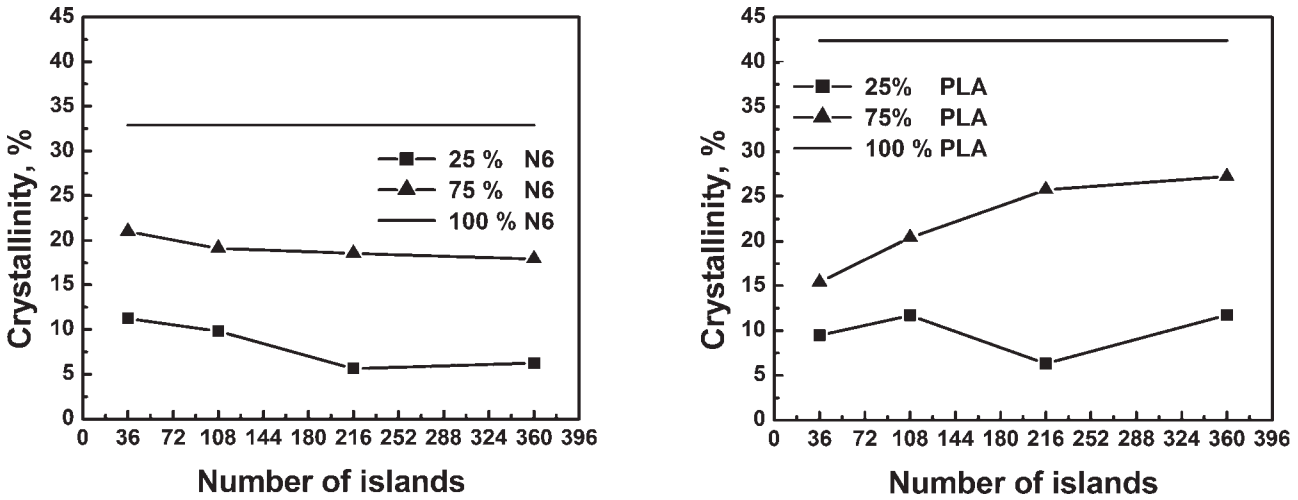

Figure 1 The crystallinity of N6 (left) and PLA (right) phases of the bicomponent and homo-component fibers as function of the number of islands for different polymer ratios.

PLA was removed in a winch beck machine. The bicomponent N6/PLA fabrics were treated for 10 min in a mixture of water and a concentration of 3% caustic soda at 100°C.

The basis weight of the bicomponent fabrics prior to the removal of PLA was kept at about 170 g/m^2. After 75 and 25% of the sea polymer was removed, the fabric basis weight dropped to 50 and 140 g/m^2, respectively.

Thermal analysis

Thermal analysis was carried out to determine the degree of crystallinity of drawn bicomponent and homo-component fibers by differential scanning calorimetry (DSC) using a PerkinElmer DSC 7 calorimeter. Standard indium sample was used to calibrate the DSC. Fibers weighing 3–4 mg were cut into thin pieces and dried overnight at 40°C. Samples were scanned at a heating rate 20°C/min between 25 and 250°C.

X-ray analysis

Wide-angle X-ray scattering (WAXS) profiles were obtained by Omni Instrumental X-ray diffractometer with a Be-filtered CuKα radiation source ($\lambda = 1.54$ Å) generated at 30 kV and 20 mA. The I/S fibers were manually wound in a tightly packed flat layer of parallel fibers onto a holder prior to the examination. The samples were equatorially scanned at the rate 0.2° min^{-1} from $2\theta = 10°$–35° in the reflection geometry. The count time was 2.5 s. Intensity curves of the equatorial scans were resolved into peaks at $2\theta = 22°$ for the N6 fibers and at $2\theta = 16.5°$ for the PLA fibers. To calculate Herman's orientation functions, transmission scans of the samples at the rate of 0.5° min^{-1} and count time 1 s at fixed diffraction angles were performed.

Mechanical properties

The tensile properties of the homo-component and bicomponent fibers were examined according to ASTM D3822-01. Twelve specimens of each sample were used to determine an average breaking force and elongation at break. The tensile properties of all fabrics were determined according to ASTM D5035. Six specimens (2.54 × 10.16 cm^2) of each sample were tested in the machine (MD) and cross-machine (CD) directions, respectively. The tear strength of the fabrics was determined according to ASTM 5733. Five specimens (7.62 × 15.24 cm^2) of each sample were tested in MD and CD, respectively, and their average values of strength were then calculated. All samples were conditioned for at least 24 h at 65% ± 2% relative humidity and temperature of 21°C ± 1°C prior to each test.

Fiber diameter measurements

The fiber diameters were obtained from micrographs of the fabrics by using image analysis system developed at NCRC. Micrographs were obtained on a Hitachi *S*-3200*N* Scanning Electron Microscope. Prior to scanning, all specimens were coated with a layer of AuPd using a Denton Vacuum Sputter Coater.

RESULTS AND DISCUSSION

Fiber properties—Crystallinity and crystalline orientation

Figure 1 highlights the relationships between the number of islands and crystallinity of the N6 and PLA

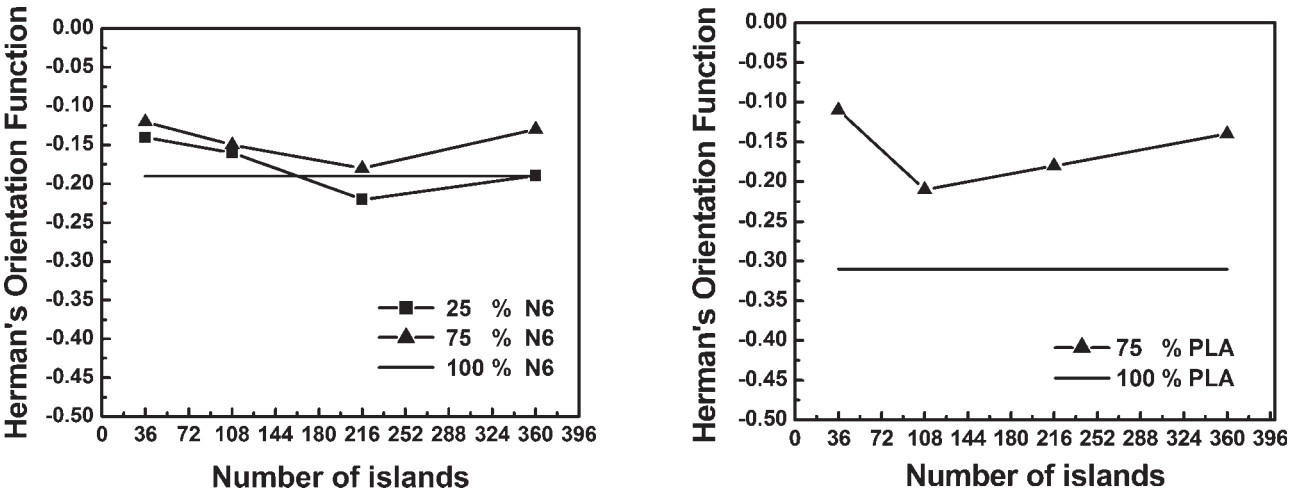

Figure 2 Crystalline orientation of the polymer chains in the N6 (left) and PLA (right) phases of the bicomponent and homo-component fibers as function of the number of islands for different polymer ratios.

phases in the I/S fibers. Bicomponent fibers made up of 36 islands showed the highest crystallinity for the N6 component, which decreased slightly as the number of islands increased from 36 to 360. On the other hand, the fibers with 360 islands exhibited the highest degree of crystallinity for the PLA phase. Overall, the crystallinities of both components of the I/S fibers were lower than the crystallinities of pure N6 and PLA fibers. Choi and Kim[22] also observed a decline in the phase crystallinity of the I/S bicomponent filaments and concluded that this decline was due to the interface between the polymers forming the bicomponent fibers.

The Herrman's orientation functions for the N6 and PLA phases of the I/S fibers as functions of the number of islands are presented in Figure 2. The Herrman's orientation function of the N6 component declined as the number of islands increased from 36 to 216. Further increases in the island count from 216 to 360 caused an increase in the crystalline orientation function of the N6 phase. The 108 I/S fibers demonstrated the lowest Herrman's orientation function of the PLA component, and this function increased as the number of islands composing the bicomponent fibers increased from 108 to 360. Fibers containing 36 islands demonstrated the highest values of the Herrman's orientation functions for both phases. Overall, the N6 and PLA components of the bicomponent fibers as well as 100% N6 and PLA fibers showed low orientation of their polymer chains in the crystalline regions. However, the axial alignment of the component polymer chains was found to be better than the alignment of the polymer chains of the homo-component N6 and PLA fibers along the fiber axis.

The bicomponent configuration quite possibly affected the solidification kinetics of both materials. We believe that the N6 islands solidified faster than the PLA sea and 100% N6 fibers in the spunbond spin-

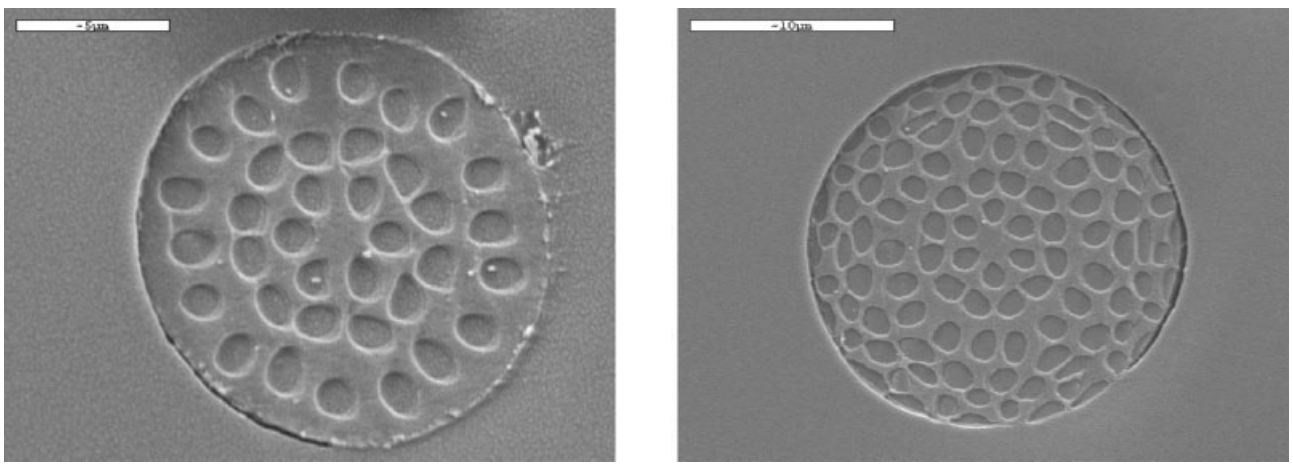

Figure 3 SEM images of cross sections of the 36 I/S N6/PLA (left) and 108 I/S N6/PLA (right) fibers: scale bars correspond to 5 (left) and 10 (right) μm.

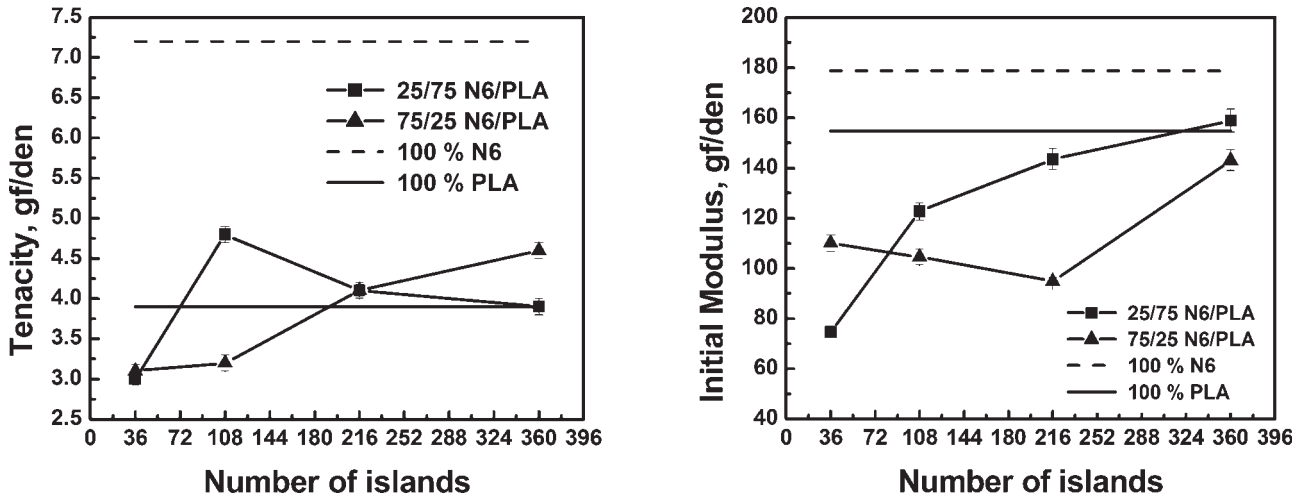

Figure 4 Tenacity (left) and initial modulus (right) of the I/S N6/PLA fibers as function of the number of islands for different polymer ratios.

line. Therefore, the N6 islands would be expected to experience higher spin-line stresses and thus, develop better molecular orientation than the 100% N6 fibers or PLA sea.[22–27] Moreover, the N6 islands would also reach final fiber spinning speed faster than the PLA phase of the I/S fibers.[22–27] Thus, N6 could promote attenuation of the PLA phase as the result of shearing forces acting on the interface between the polymers.[27] This could be a reason for an improvement of the PLA phase crystalline orientation compared with that of the PLA homo-component fiber. Similar arguments may be used to explain the Herrman's orientation functions observed for the PLA and N6 components in the 36 I/S fibers. These fibers demonstrated the most uniform distribution of the islands over the filament cross sections (Fig. 3). Such distribution could lead to a better, even attenuation of the PLA and N6 phases due to the shearing forces acting on their interface and result in a higher values of the Herrman's orientation function of these components. On the other hand, the bicomponent fibers with 108 or higher island count demonstrated uneven distribution of the islands over the fiber cross sections, as can be seen from Figure 3. This could prevent an equal drawing of the PLA and N6 components in the spunbond spinline and result in the decline of the component crystalline orientation. It is also probable that 108 and 216 I/S fibers had the most uneven distribution of the islands over the fiber cross section, which could result in a drop in the values of Hermann's orientation function of the PLA and N6 components composing these fibers.

Fiber mechanical properties before and after PLA removal

Tensile properties of the composite I/S fibers (without removing PLA) are reported in Figure 4. With the

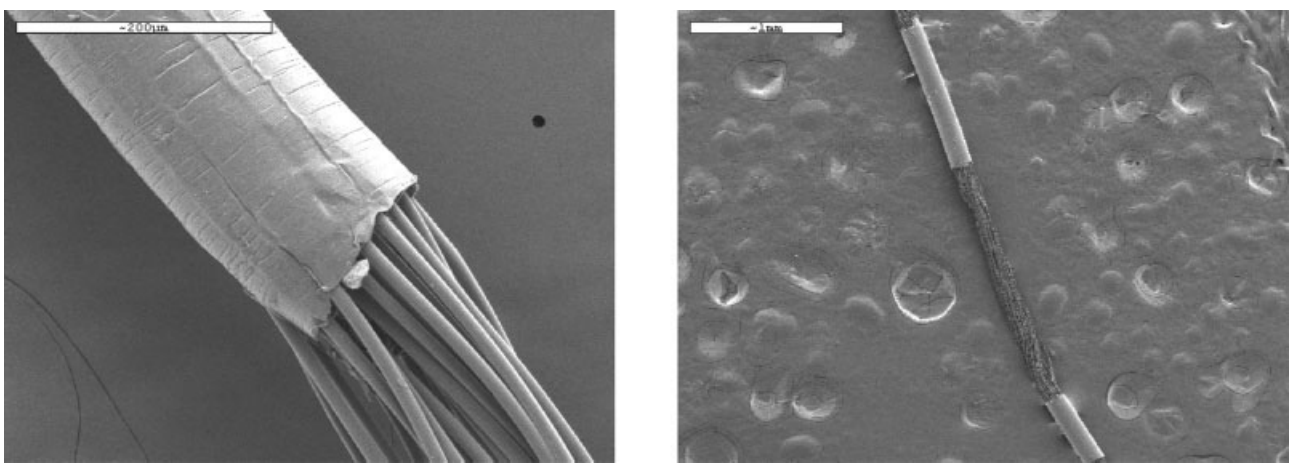

Figure 5 SEM images of the N6/PLA I/S fiber fracture under the load: scale bars correspond to 200 (left) and 1000 (right) μm.

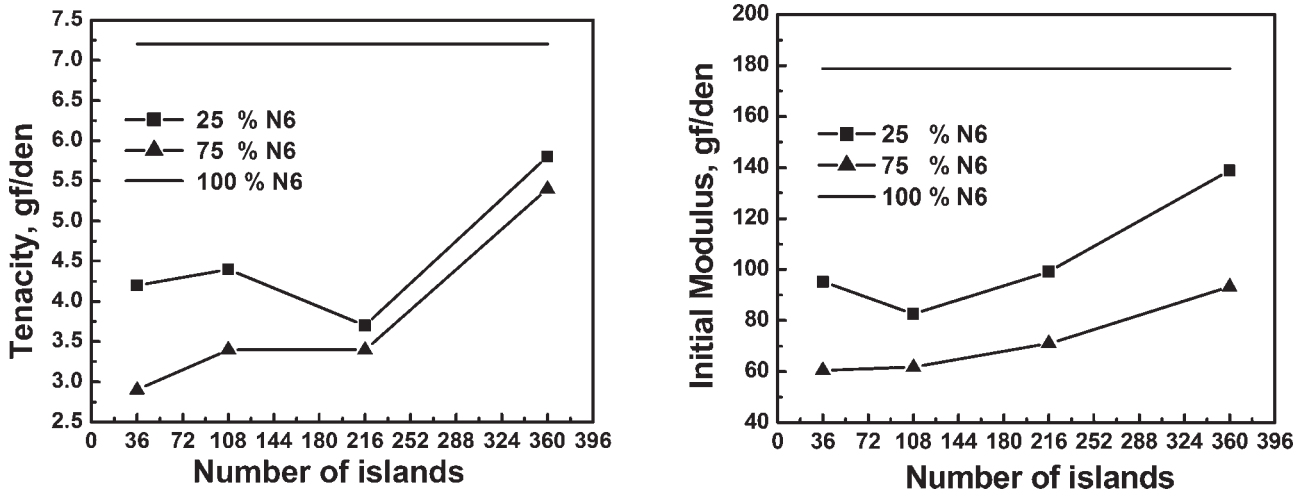

Figure 6 Tenacity (left) and initial modulus (right) of the N6 fibers after PLA removal as function of the number of islands for different polymer ratios.

exception of tenacity for the filaments with 25% N6, all fibers containing 360 islands showed the highest tenacity and initial modulus. The results reported in Figure 4 and those depicted in Figures 1 and 2, show a lack of correlation between I/S ultimate fiber properties and their crystallinity or crystalline orientation. This may suggest that amorphous orientation played a dominant role in the mechanical properties of the fibers.[28] Overall, the I/S fibers demonstrated performance similar to that of PLA homo-component filaments, which had a lower elongation to break than 100% N6 fibers. The fracture of PLA sea probably initiated the catastrophic failure of the bicomponent fibers, as shown in Figure 5. Thus, the I/S fibers tended to exhibit tensile properties similar to those of 100% PLA fibers.

After the removal of PLA from the N6/PLA I/S fibers, the tensile properties of the N6 fibers were investigated and the results are reported in Figure 6. The data suggest that the values of the fiber tenacity and initial modulus grew as the number of islands initially composed of the I/S fibers increased from 36 to 360. Somewhat similar trends were reported for the tenacity and initial modulus of the I/S N6/PLA fibers (Fig. 4).

The majority of the N6 fibers exhibited performance superior to that of the I/S fibers. Overall, the N6 fibers originally made up of 360 islands showed the highest values of the tenacity and modulus. Thus, if there is direct correlation between N6 fiber and fabric performance, the web initially composed of 360 islands would be expected to have the best mechanical properties.

Fiber diameter after PLA removal

The diameters of the N6 fibers after the removal of the sea were measured and the results are reported in Figure 7. As expected, the diameter of the N6 fibers decreased as the island count and PLA ratio in the composite I/S fibers increased. The fibers with 25% of N6 showed a decrease in fiber diameter from 1.3 to 0.36 μm when the number of islands was increased from 36 to 360. The diameter of fibers with 75% of N6 showed a decline from 2.3 to 0.5 μm for the same range. The smallest island fiber produced in this study measured 360 nm. The initial diameter of the composite fiber was 13 μm or 1.5 dpf (denier per filament). Overall, our data suggest that both micro- and nanofibers could be easily produced by using of the I/S fiber technology, however to obtain nanofibers, rather than microfibers, higher percentage ratio of the sea polymer needs to be removed or higher number of islands (252 and more) is required to be used in the original I/S configurations (Fig. 7).

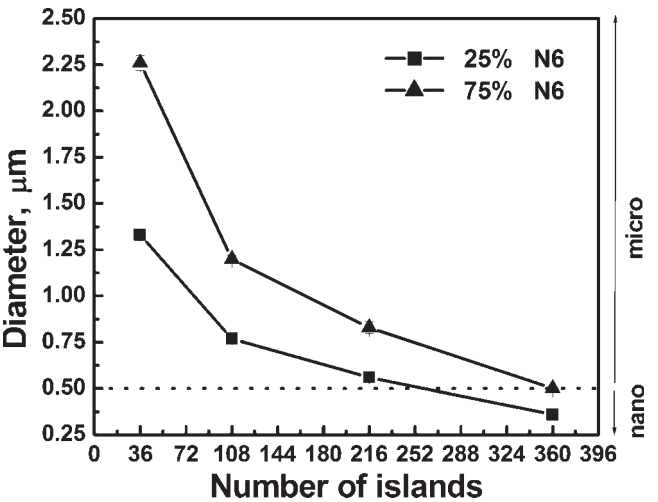

Figure 7 Diameter of the N6 fibers after PLA removal as function of the number of islands for different polymer ratios.

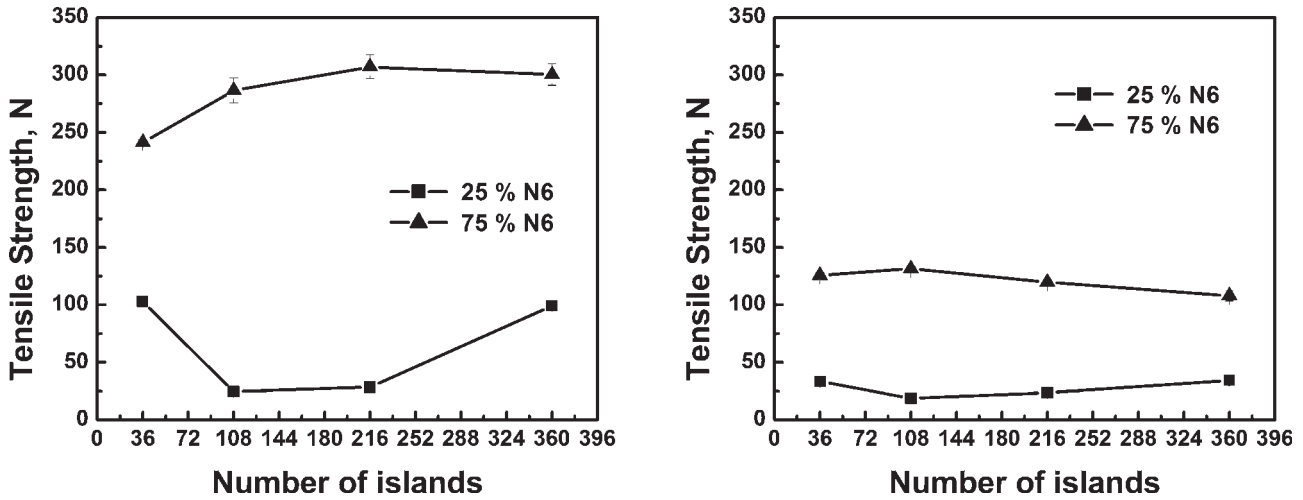

Figure 8 Tensile strength of the N6 fabrics after PLA removal in MD (left) and CD (right) as function of the number of islands for different polymer ratios.

Fabric mechanical properties after PLA removal

After PLA was removed from the hydroentangled N6/PLA fabric, tear and tensile properties of the N6 webs were obtained and the results are summarized in Figures 8 and 9. It may be noted that fabrics made up of micro- or nanofibers did not show significant differences in their values of the tensile and tear strength. This observation suggests that nonwovens examined did not show either significant deterioration or improvement in their mechanical properties as the size of the fibers comprising these webs significantly decreased. This disagrees with the results reported in Figure 6 for the N6 fibers, where the fibers originally composed of 360 islands demonstrated the best performance. The disagreement is partly due to the fact that the fabrics examined did not entangle equally well and consequently, bonding efficiency rather than fiber strength was the dominant factor influencing the fabric mechanical properties.

Among the samples made up of 75% of N6, the fabrics initially consisted of 108 and 216 islands showed the best tensile and tear performance in CD and MD, respectively. Nonwovens originally composed of 25% of N6 and 36 islands demonstrated the highest tensile and tear properties in MD, whereas the webs made up of 25% of N6 and 360 islands had the highest values of the tensile and tear strength in CD. Visual examination of the hydroentangled substrates, which exhibited the best performance, suggested that these webs had the most uniform structure and showed no delaminating during mechanical testing in contrast to other samples examined. This means that web uniformity and bonding efficiency were prevalent factors

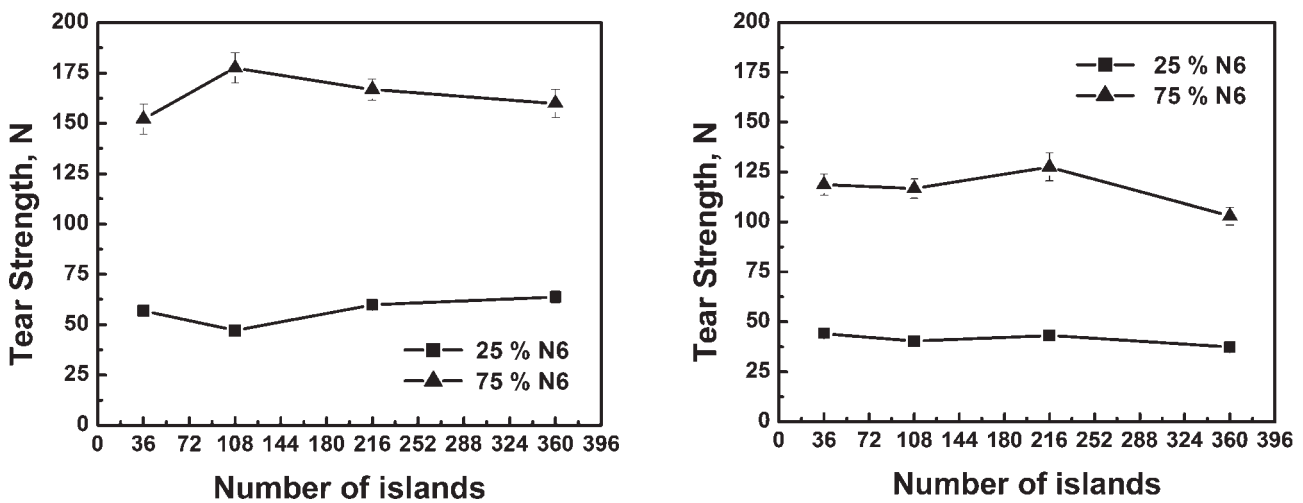

Figure 9 Tear strength of the N6 fabrics after PLA removal in MD (left) and CD (right) as function of the number of islands for different polymer ratios.

TABLE III
Tensile and Tear Properties of the N6 Fabric Originally Composed of 108 Islands

		MD		CD	
No.	Bonding conditions	Tensile strength (N)	Tear strength (N)	Tensile strength (N)	Tear strength (N)
1	Hydroentangled only – PLA removed	168.7 ± 4.8	83.4 ± 3.5	51.0 ± 2.4	151.1 ± 3.5
2	Hydroentangled and calendered at 145°C after PLA removal	178.5 ± 6.8	49.1 ± 2.6	52.0 ± 0.4	104.0 ± 4.0
3	Hydroentangled and calendered at 190°C prior to PLA removal	69.7 ± 3.2	27.5 ± 1.3	29.4 ± 0.8	43.2 ± 1.7

influencing the mechanical properties of the hydroentangled N6 webs.

To compare the performance of the 75% N6 and 25% N6 webs, their strength were normalized to the same basis weight (100 g/m^2). The normalized data displayed insignificantly small differences between the strength of 25% N6 and that of 75% N6 webs and these differences resulted from dissimilarities in the web structure and uniformity.

Overall, the hydroentangled N6 fabrics consisting of micro- and nanofibers showed high values of both tensile and tear strength compared with those of commercially available fabrics of similar construction. For instance, Evolon nonwovens, consisting of microfibers measuring about 2.5 μm and having basis weight of 100 g/m^2, have tensile strength of 250 N/5 cm, which is comparable to the tensile strength of the examined N6 micro- and nanowebs.[21] Such observation is expected because Evolon nonwovens are typically made up of larger fibers than the N6 fabrics. However, the tear strength of the Evolon web is only in the range from 6 to 10 N, which is significantly lower than the tear strength of the examined N6 nonwovens.[21]

The tensile properties of the N6 hydroentangled fabrics composed of micro- and nanofibers were slightly improved by calendering of these webs after PLA removal, as shown in Table III. The improvement in the N6 web tensile strength is likely due to an increase in the fabric stiffness, which in turn, enhances fabric resistance to an applied stress and increases the amount of force needed to cause the fabric failure. However, the tear strength of the N6 hydroentangled nonwovens after point-bonding was reduced significantly, which is mostly due to the reduced mobility of the fibers as it was reported by Bhat et al.[29,30] Thus, calendering of the N6 hydroentangled fabrics does not offer significant advantages with respect to the tensile strength and leads to a lower tear resistance. However, if the N6 web pilling and abrasion resistance needs to be significantly improved for their use in some applications, this could be done by calendering of the hydroentangled substrates after PLA removal. Calendering typically ties down the fibers on the fabric surface and improves web performance in terms of its pilling and abrasion resistance.

The hydroentangled N6 webs, which were thermally point-bonded before PLA removal, showed

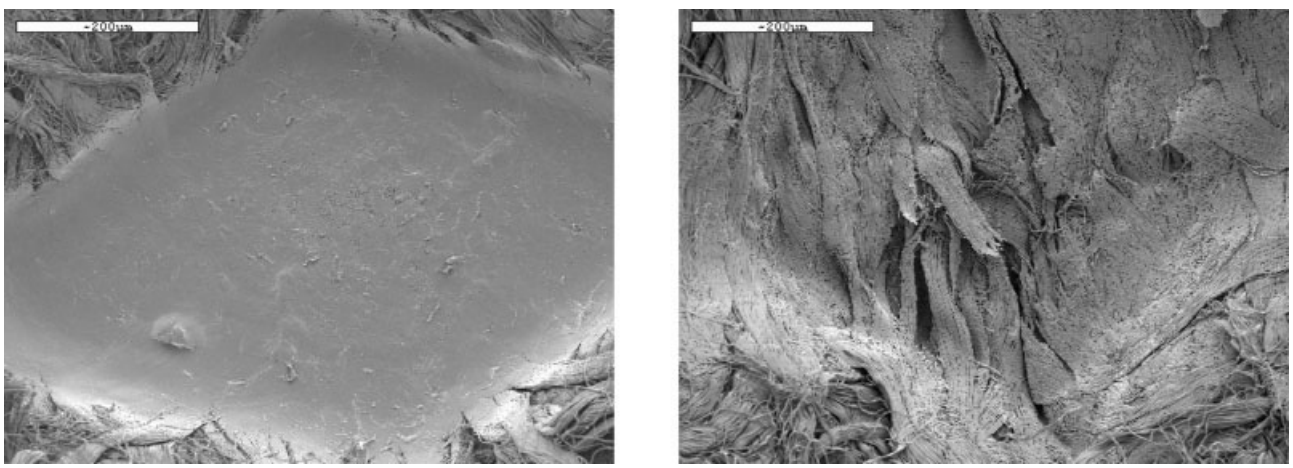

Figure 10 SEM micrographs of the bond spots of the I/S hydroentangled fabric: point-bonded after PLA removal (left) and point-bonded before PLA removal (right): scale bars correspond to 200 μm.

poor performance after the sea was dissolved. Calendering of the bicomponent webs at 190°C caused interdiffusion of N6 and PLA polymers in the fibers forming bond spots. Thus, the removal of PLA led to the disintegration of the bonds that became a source of the N6 fabric failure under the stress (Fig. 10). This suggests calendering as inappropriate method of bonding of the I/S structures. On the other hand, hydroentangling was shown to be the preferred method of bonding of such bicomponent structures, because of its ability to withstand the postprocessing steps required for dissolving of the sea from the I/S nonwovens.

CONCLUSIONS

In this study we demonstrated the utility of the spunbond process for the production of relatively high strength micro- and nanofiber based nonwovens. It was shown that micro- and nanofiber webs with low basis weights and high strength could be produced by the spinning of the I/S fibers made up of N6 (islands) and PLA (sea) with the subsequent removing of PLA. We demonstrated that hydroentangling was the preferred method of bonding of these bicomponent structures and that the hydroentangled fabrics, in contrast to thermally bonded samples, were able to withstand postprocessing steps required for dissolving of the sea from the resulting nonwovens. Overall, filaments as small as 360 nm were obtained by removing of 75% of PLA from the bicomponent fibers containing 360 islands and having the initial diameter of 13 μm (1.5 dpf).

An investigation of the role of the number of islands and percent polymer composition on the N6 fiber properties showed that an increase in the island count or the sea polymer content caused a decrease in the resulting fiber diameter and improvements in its mechanical properties. On the other hand, the island count or polymer percent composition did not have a significant effect on the performance of the N6 fabrics after the PLA phase was removed.

The best mechanical properties demonstrated hydroentangled N6 webs that had the most uniform structure and were bonded most efficiently. Thus, bonding and web uniformity were found to be a dominant factors influencing fabric performance.

Overall, the N6 fabrics composed of micro- and nanofibers demonstrated high values of the tensile and tear strength, suggesting that the I/S approach is a promising technique for the production of high strength micro- and nanofiber webs. Nonetheless, the question remains whether or not it is possible to obtain strong micro- and nanofiber based nonwovens by using different polymer combinations. This issue will be addressed in a subsequent paper.

The generous support of Nonwovens Cooperative Research Center is gratefully acknowledged. Polymers for this study were provided by BASF and Nature Works LLC.

References

1. Graham, K.; Gogins, M.; Schreuder-Gibson, H. Int Nonwovens J 2004, 13, 21.
2. Subbiah, T.; Bhat, G. S.; Tock, R. W.; Parameswaran, S.; Ramkumar, S. S. J Appl Polym Sci 2005, 96, 557.
3. Sun, Z.; Zussman, E.; Yarin, A. Y.; Wendorff, J. H.; Greiner, A. Adv Mater 2003, 15, 1929.
4. Grafe, T.; Gogins, M.; Barris, M.; Schaefer, J.; Canepa, R. Presented at Filtration International Conference and Exposition of the INDA, Chicago, IL, Dec. 3–5, 2001.
5. Baker, B. Int Fiber J 1998, 13, 26.
6. Grafe, T.; Graham, K. Int Nonwovens J 2003, 12, 51.
7. Cheng, K.-K. Int Fiber J 1998, 13, 40.
8. Okamoto, M. U.S. Pat. 4,127,696 (1978).
9. McCann, J. T.; Li, D.; Xia, Y. J Mater Chem 2005, 15, 735.
10. MacDiarmid, A. G.; Jones, W. E., Jr.; Norris, I. D.; Gao, J.; Johnson, A. T. Jr.; Pinto, N. J.; Hone, J.; Han, B.; Ko, F. K.; Okuzaki, H. Synth Met 2001, 119, 27.
11. Kessick, R.; Tepper, G. Appl Phys Lett 2003, 83, 557.
12. Reneker, D. H.; Chun, I. Nanotechnology 1996, 7, 216.
13. Zhang, D.; Sun, C.; Song, H. J Appl Polym Sci 2004, 94, 1218.
14. Zhao, R.; Wadsworth, L. C. Polym Eng Sci 2003, 43, 463.
15. Fabbricante, A.; Ward, G.; Fabbricante, T. U.S. Pat. 6,114,017 (2000).
16. Hagewood, J. Int Fiber J 1998, 13, 47.
17. Li, D.; Xia, Y. Adv Mater 2004, 16, 1151.
18. Bresee, R. R.; Ko, W.-C. Int Nonwovens J 2003, 12, 21.
19. Bresee, R. R.; Qureshi, U. A.; Pelham, M. C. Int Nonwovens J 2005, 14, 11.
20. Zhao, R.; Wadsworth, L. C.; Sun, C.; Zhang, D. Polym Int 2003, 52, 133.
21. Groten, R.; Grissett, G. Presented at TechTextil Symposium, Atlanta, GA, March 27–30, , 2006.
22. Choi, Y. B.; Kim, S. Y. J Appl Polym Sci 1999, 74, 2083.
23. Kikutani, T.; Radhakrishnan, J.; Arikawa, S.; Takaku, A.; Okui, N.; Jin, X.; Niwa, F.; Kudo, Y. J Appl Polym Sci 1996, 62, 1913.
24. El-Salmawy, A.; Miyamoto, M.; Kimura, Y. Text Res J 2000, 70, 1011.
25. Cho, H. H.; Kim, K. H.; Kang, Y. A.; Ito, H.; Kikutani, T. J Appl Polym Sci 2000, 77, 2254.
26. Rwei, S. P.; Jue, Z. F.; Chen, F. L. Polym Eng Sci 2004, 44, 331.
27. Yoshimura, M.; Iohara, K.; Nagai, H.; Takahashi, T.; Koyama, K. J Macrmol Sci Phys 2003, 42, 325.
28. Yamada, K.; Kamezawa, M.; Takayanagi, M. J Appl Polym Sci 1981, 26, 49.
29. Bhat, G. S.; Malkan, S. R. J Appl Polym Sci 2002, 83, 572.
30. Bhat, G. S.; Jangala, P. K.; Spruiell, J. E. J Appl Polym Sci 2004, 92, 3593.